Earthquake Hazard Research in the Greater Los Angeles Basin and Its Offshore Area

#14-08-0001-A0620
Ta-liang Teng and Thomas L. Henyey
Center of Earth Sciences
University of Southern California
Los Angeles, CA 90089-0740
(213) 740-5838

INVESTIGATION

Monitor earthquake activity in the Los Angeles Basin and the adjacent offshore area. Upgrade instrumentation by installing large dynamic telemetry systems and deploying downhole seismometers. Carry out waveform analysis for crustal anisotropy and stress field determination. Investigate the reflected and converted phases to delineate the Los Angeles basin-basement contact.

RESULTS

During 1990, a total of 690 earthquakes were located in the Los Angeles basin and its offshore area. The February 28, 1990 Upland sequence with a M=5.5 main shock accounts for more than half of the events recorded in 1990. In the meantime, Santa Monica bay, the Newport-Inglewood fault, and the Whittier fault and its NW extension have been seismically active. Figure 1 shows the 1990 seismicity in the greater Los Angeles basin. About 95% of the reported 1990 events have magnitudes less than $M_L = 3.0$. A total of 36 events have $M_L \geq 3.0$. The number of earthquakes per day in the Los Angeles basin during 1990 is shown in Figure 2. The large peak beginning on February 28 corresponds to the Upland earthquake sequence. The detection threshold and location precision are being improved constantly. Figure 3 gives the capability of the Los Angeles Basin Seismic Network's (LABNET) current resolutions on epicenter and focal depth.

The continued increase in the number of recorded earthquakes can be explained in part by the improvement of the seismic network coverage that allows lowering of the detection threshold with more precise locations. But an overall increase of seismic activity in the Greater Los Angeles area has been recognized in the recent past. The October 17, 1987 Whittier Narrows earthquake ($M_L = 5.9$) was followed by a very long aftershock sequence with a large number of events that lasted well into 1988; this activity has not died out completely, even in 1990. Meanwhile, the first Upland sequence occurred on June 26, 1988 with a main shock $M_L = 4.6$. A large swarm occurred in Santa Monica bay on January 19, 1989, some 25 km off the coast south of Malibu, with main shock $M_L = 5.0$; this activity is still on-going during 1990. During this reporting period, an even larger swarm, the second Upland sequence, occurred on February 28, 1990 with main shock $M_L = 5.5$. This second Upland sequence was very strong; it consisted of at least three large aftershocks in the range of $M_L = 4.6$-4.7 and the aftershocks accounted for more than half of the recorded and located events in 1990. The two Upland sequences form a NE-trending aftershock zone; this orientation is more obvious from the fault-plane solutions. Both sequences are believed to have occurred on a NE-trending fault that undergoes left-lateral strike-slip movement.

The mechanisms of four Upland events are given by their fault-plane parameters:

		Magnitude	Strike	Dip	Rake
1.	February 28, 1990	M = 5.5	310	70	0
2.	March 1, 1990	M = 4.7	316	70	349
3.	March 2, 1990	M = 4.6	295	75	10
4.	April 17, 1990	M = 4.6	315	70	0

All four fault planes are very consistent, showing left-lateral strike-slip motions.

A shear-wave splitting analysis was performed using seismic waveform data. The result is interpreted in terms of microcrack distribution and orientation in the upper crust. Figure 4 gives a sample of the shear-wave splitting data and the associated particle diagram. It is found that microcracks in the Los Angeles basin are oriented NS and nearly vertical, with a crack density between 0.04 ~ 0.06. This implies a NS regional compression operative in the Los Angeles basin area. However, close to the thrust fault regions, such as along the Palos Verdes fault and the Malibu-Santa Monica fault, the microcrack orientation may turn sub-horizontal due to the thrust motion. A stress mapping summary is given in Figure 5 with the solid dots with thick arrows showing the crack of stress orientation.

V. REFERENCES

Chiu, H.C., Kuo, J.H., and Teng, T.L.(1990) Recovery of source function from surface observation: A SH line source under a semi-cylindrical canyon, EOS, 71, 43, p. 1459.

Li, S.B., and Teng, T.L. (1990) Dependence of Richter magnitude scale on site condition and local geology, EOS, 71, 43, p.1471.

Li, Y.G., Teng, T.L., and Henyey, T.L.(1991) A Shear-wave Splitting Analysis of the Los Angeles Basin based on Network Data, to be submitted.

Hauksson, E. (1987). Seismotectonics of the Newport-Inglewood fault zone in the Los Angeles Basin, southern California, Bull. Seism. Soc. Am., 77, 539-561.

Hauksson, E., L. M. Jones, T. L. Davis, L. K. Hutton, G. Brady, P. A. Reasenberg, A. J. Michael, R. F. Yerkes, P. Williams, G. Reagor, C. W. Stover, A. L. Bent, A. K. Shakal, E. Etheredge, R. L. Porcella, C. G. Bufe, M. J. S. Johnston, E. Cranswick (1988), The 1987 Whittier Narrows Earthquake in the Los Angeles Metropolitan Area, California, Science, 239, 1403-1412.

Su, F., Koyanagi, S., Zeng, Y.H., Mayeda, K., Teng, T.L., and Aki, K. (1990) A recursive stochastic inversion of site effect using coda waves, EOS, 71, 43, p. 1474.

Teng, T. L. and T. L. Henyey (1973). Microearthquake monitoring in the City of Long Beach area for the year 1972, U.S.C. Geophysics laboratory Tech. Rpt. No. 73-2, Los Angeles, CA.

Teng, T.L., and Wang, (1990) Analysis of short-period waveform in the Los Angeles basin, OES, 71,43, p. 1474.

Teng, T.L., and Li, S.B.(1991) Reflections from the basin-basement contact of the Los Angeles basin from strong motion data, in preparation.

Ziony, J. I. and R. F. Yerkes, (1985). Evaluating earthquakes and surface-faulting potential, U.S. Geological Survey Prof. paper 1360, 43-91.

LOS ANGELES BASIN EARTHQUAKES

January – December 1990

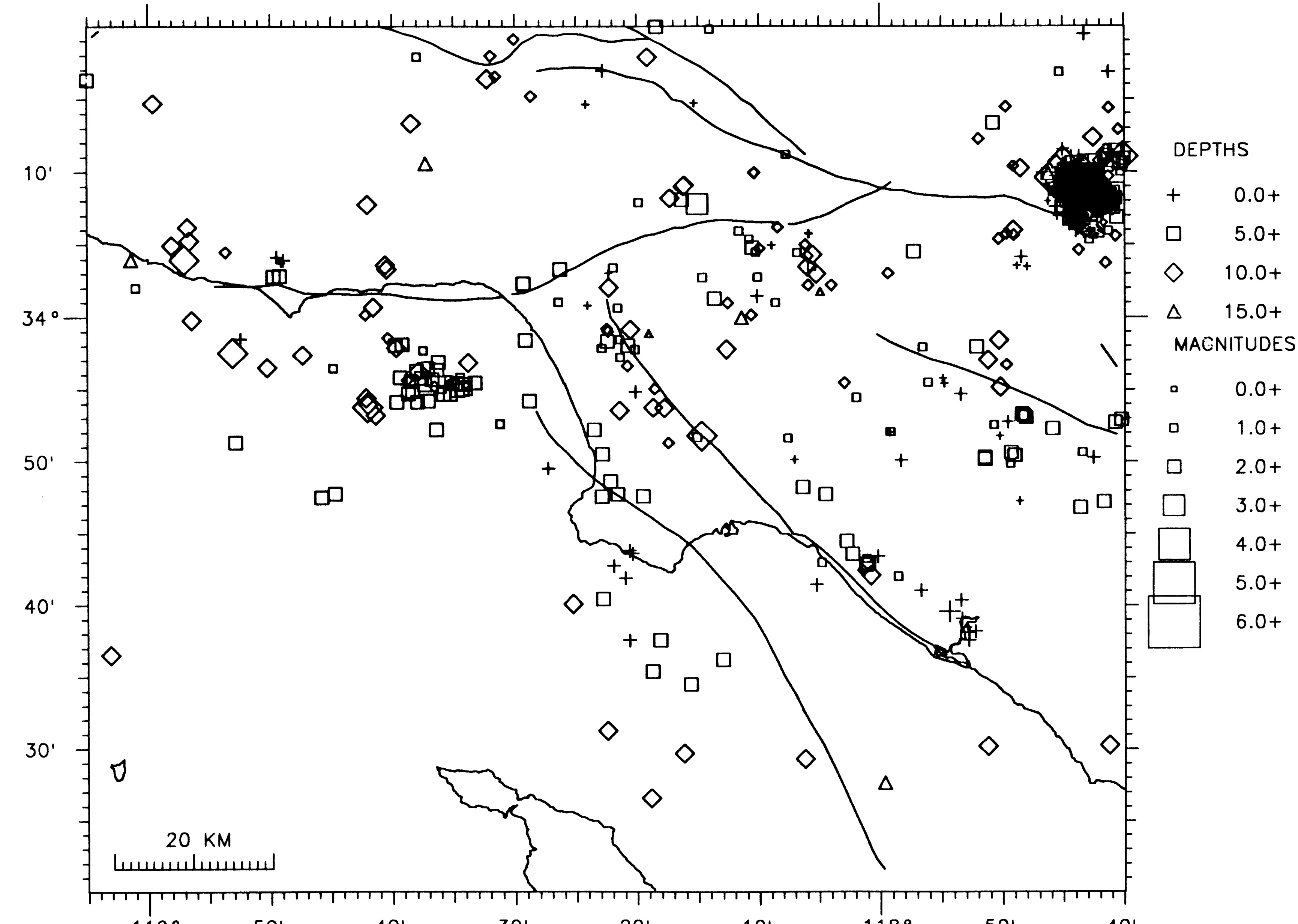

Figure 1.

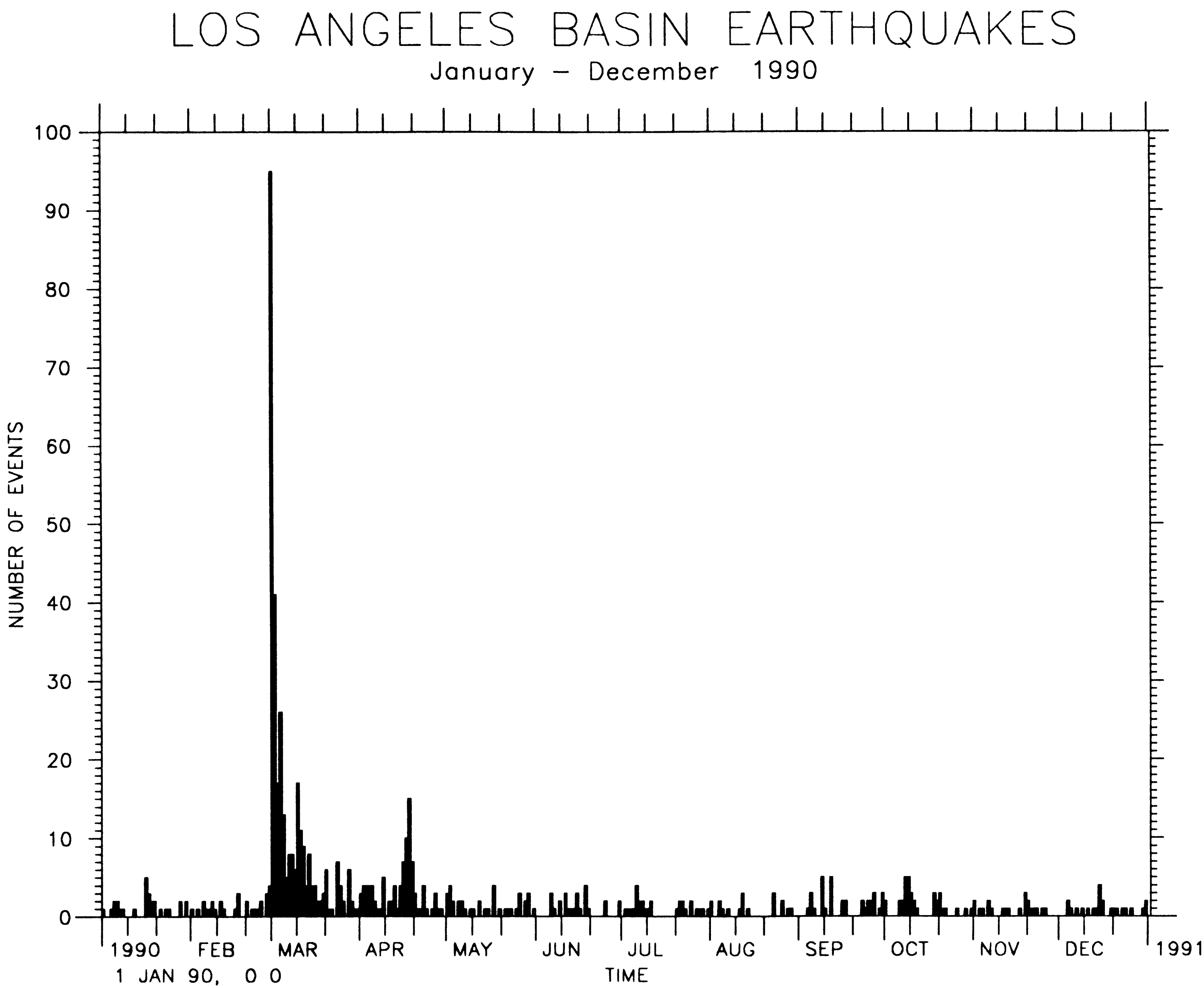
LOS ANGELES BASIN EARTHQUAKES
January – December 1990
NUMBER OF EVENTS
0
10
20
30
40
50
60
70
80
90
100
1990
FEB
MAR
APR
MAY
JUN
JUL
AUG
SEP
OCT
NOV
DEC
1991
1 JAN 90, 0 0
TIME

Figure 2.

HYPOCENTER UNCERTAINTY UXY00

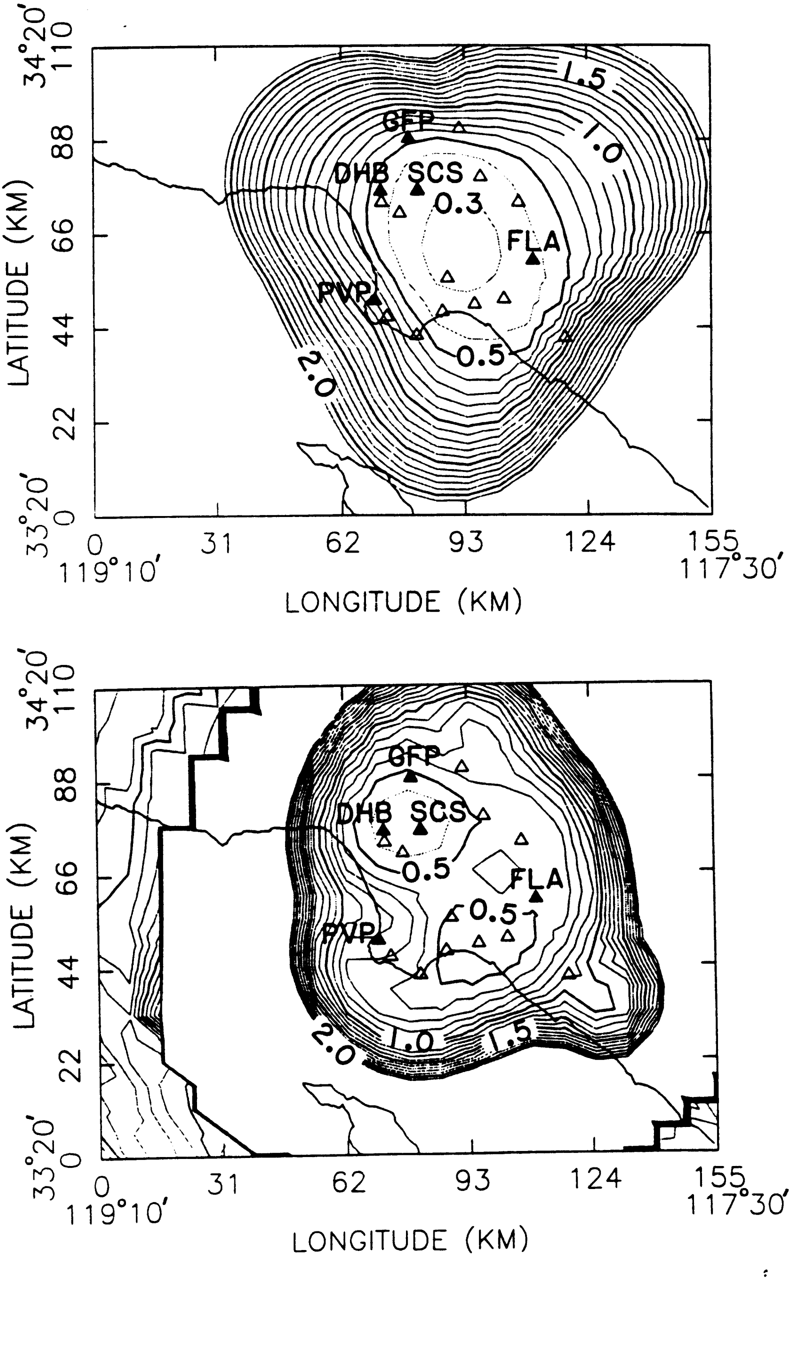

Figure 3.

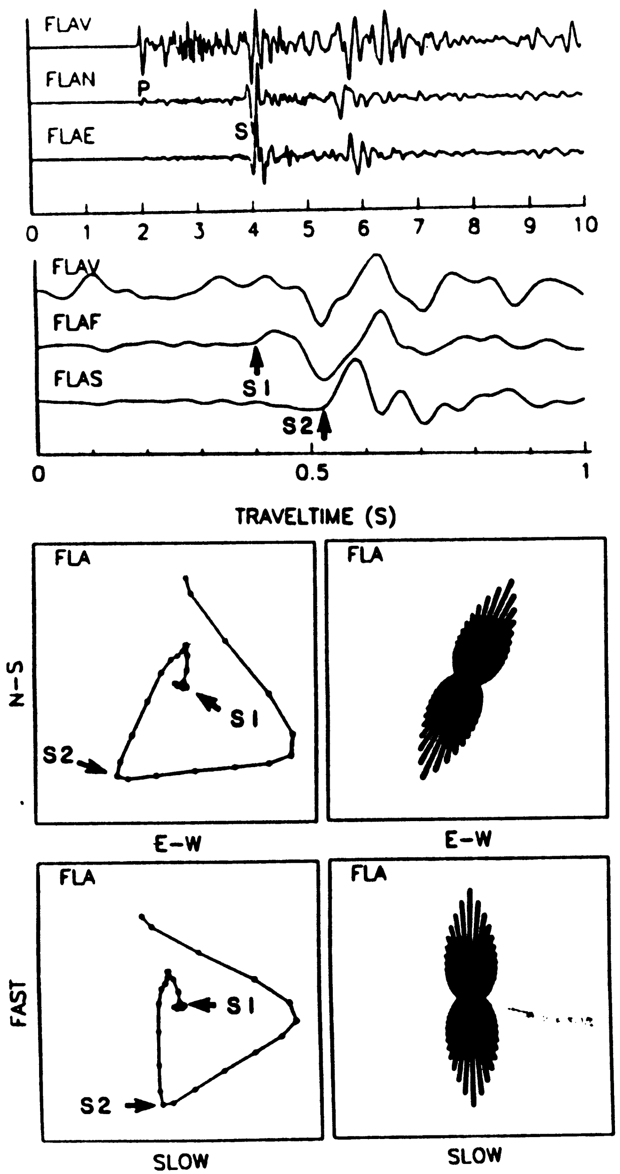

Figure 4a.

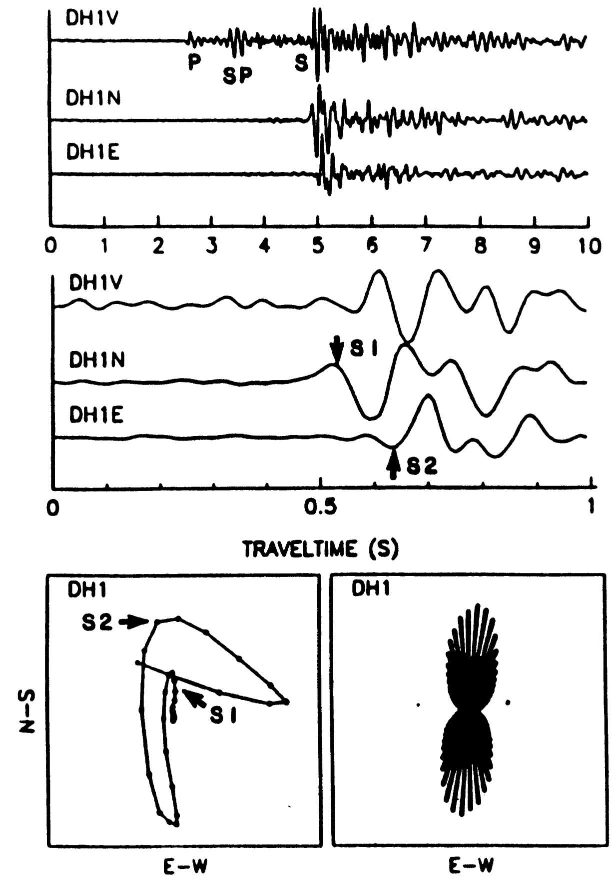

Figure 4b.

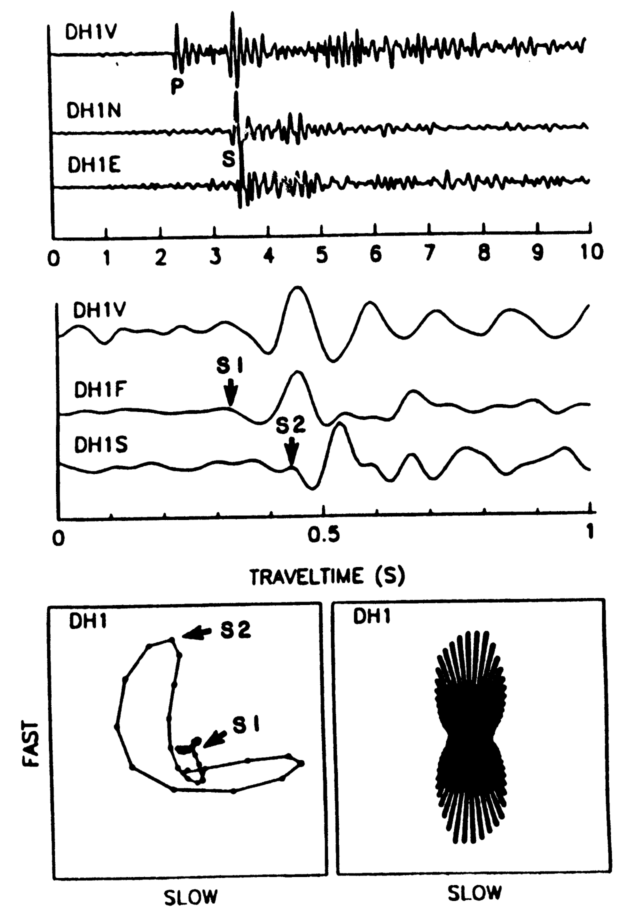

Figure 4c.

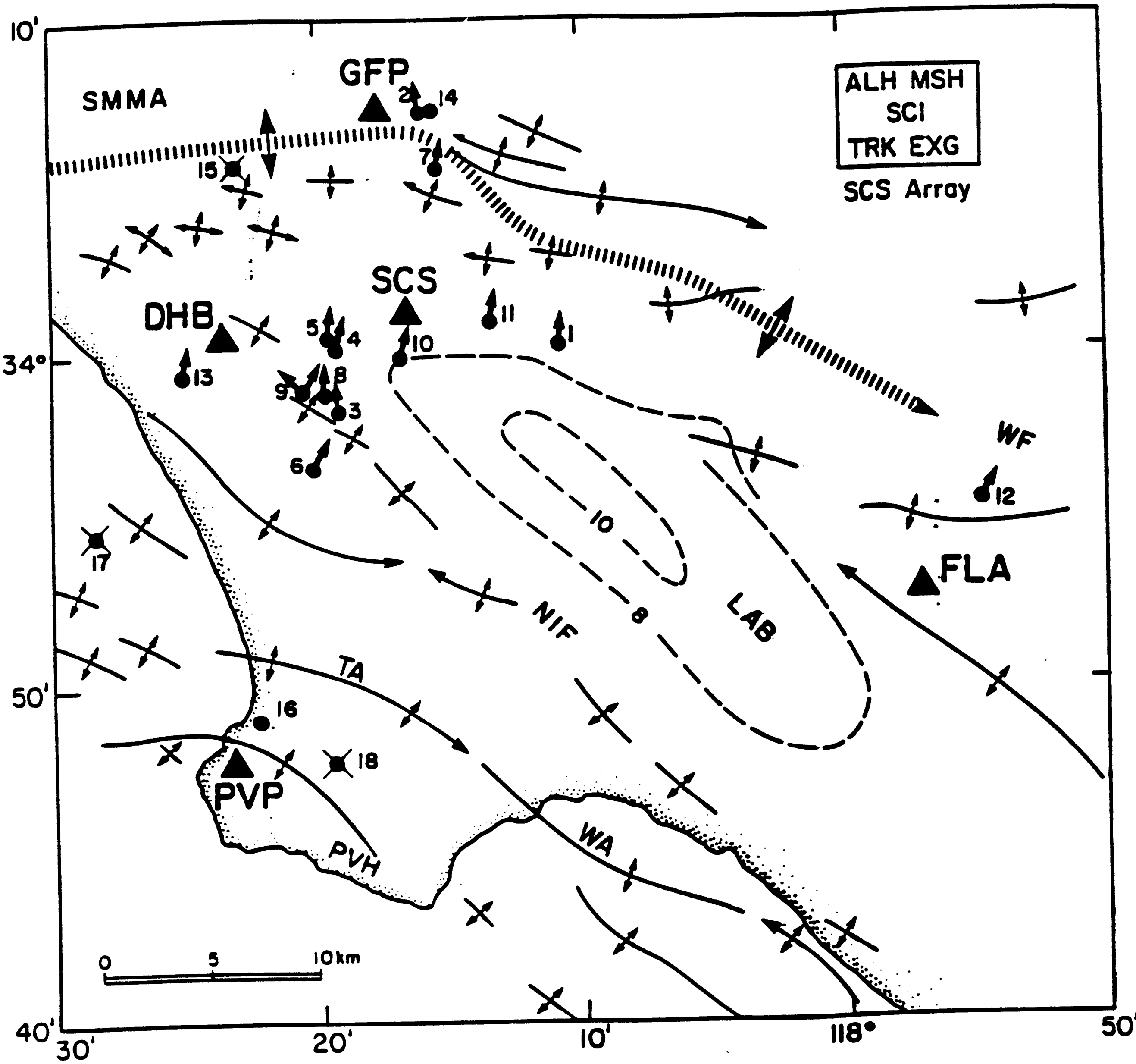

10'
34°
50'
40'
30'
20'
10'
118°
50'
SMMA
GFP
SCS
DHB
PVP
FLA
ALH MSH
SCI
TRK EXG
SCS Array
WF
NIF
LAB
TA
WA
PVH
10
8
1
2
3
4
5
6
7
8
9
10
11
12
13
14
15
16
17
18
0
5
10km

Figure 5.